



The Space Congress® Proceedings

1968 (5th) The Challenge of the 1970's

Apr 1st, 8:00 AM

Determining the Magnetism of Small Spacecraft

M. H. Lackey

U. S. Naval Ordnance Laboratory White Oak, Maryland

Follow this and additional works at: <https://commons.erau.edu/space-congress-proceedings>

Scholarly Commons Citation

Lackey, M. H., "Determining the Magnetism of Small Spacecraft" (1968). *The Space Congress® Proceedings*. 1.

<https://commons.erau.edu/space-congress-proceedings/proceedings-1968-5th/session-11/1>

This Event is brought to you for free and open access by the Conferences at Scholarly Commons. It has been accepted for inclusion in The Space Congress® Proceedings by an authorized administrator of Scholarly Commons. For more information, please contact commons@erau.edu.

EMBRY-RIDDLE
Aeronautical University™
SCHOLARLY COMMONS

DETERMINING THE MAGNETISM OF SMALL SPACECRAFT

by M. H. Lackey
U. S. Naval Ordnance Laboratory
White Oak, Maryland

Introduction

A satellite has permanent magnetism associated with it resulting from the magnetization of ferrous items distributed about its volume. The magnetism will interact with the earth's magnetic field producing a torque about the center of gravity of the satellite. If this torque is large, it can misalign the satellite and cause it to oscillate in its orbit. Prior to launch the magnetic field from the permanent magnetism can be measured and analyzed to determine how much torque will be produced by an external magnetic field. Ideally there exists some dipole moment called the "effective or resultant dipole moment of the satellite," which produces an equivalent interaction with respect to torque in the earth's magnetic field.

This paper contains a general discussion of the process for defining the effective dipole moment of a satellite. Illustrations are included to clarify the discussion. A description is given of the coil facility in which the magnetic testing is accomplished and of the method for measuring the magnetic field of the satellite. Parameters that affect the measurements are described, e.g., the effect of instrument sensitivity and distance of measurement on the smallest measurable dipole moment. Basic analysis procedures are discussed, and possible methods for improving and extending the procedures are given. Computer generated curves are included as examples of typical measurement data. No attempt is made in this paper to provide thorough mathematical details although mention is made of harmonic analysis techniques and methods of least squares approximation. The purpose herein is to survey the general procedures for measuring and analyzing the magnetism of satellites.

Coil Facility

The Naval Ordnance Laboratory (NOL) has coil facilities in which background magnetic fields can be set up in any direction with amplitudes from 0 to 600 millioersted. The background field is uniform to better than 0.1 percent over a sphere eight feet in diameter. The stability of the field is better than ± 2 gamma for typical measurement periods (2 to 3 minutes). The facility generally used for spacecraft testing contains a 24-foot cubical coil system as shown in Figure 1. The system contains coils for generating fields along three orthogonal axes. There are two independent coils for each axis. The magnetic axis for the x-coils is horizontal and parallel to magnetic north. The magnetic axis for the y-coils is

horizontal and perpendicular to magnetic north. The number of turns in each coil segment has been adjusted to give optimum uniformity in the generated field. The center z-coil segment is pivoted to permit items with diameters as large as eight feet to be placed inside the coil system. The facility contains a 6 x 8 foot concrete monolith. The top of the monolith is even with the floor at five feet two inches below the center of the coil system. This allows heavy items to be tested with rigid support.

The sensitivity of the test facility is in the range of 1 to 4 gamma. This sensitivity, along with the measurement distance, determines the smallest measurable dipole moment. Figure 2 shows this relationship for a sensitivity of 4 gamma when the axial field of the dipole is considered. The vertical scale has been increased to extend the range of the curve. For measurements at a distance of 4 feet the smallest measurable dipole moment is about 18 gauss-cm³. For 10 feet the value is 283 gauss-cm³.

Measurement Techniques

Facility equipment for measuring and recording components of the magnetic field includes magnetometers, an xy-recorder and a turntable. Voltage outputs from a magnetometer and the turntable feed the xy-recorder producing graphs representing a component of the magnetic field versus the turntable rotation angle. The measurements can be recorded with a sensitivity of 10 gamma/inch and 30°/inch. For future measurements a gimballing structure will be needed to give a tilt axis as shown in Figure 3. This will provide the 2 degrees of freedom necessary for adequate data. The coordinate axes for the satellite are initially aligned as shown. With this orientation the measurements can easily be identified by the spherical coordinates (r, θ, ϕ) where r is the measurement distance, θ is the azimuth or tilt angle, and ϕ is the zenith or rotation angle.

Measurements are made of the normal component of the magnetic field on the surface of a sphere surrounding the satellite. Sensitive magnetometers are used to determine the measurement data while the satellite is in a zero magnetic environment. At positions close to the satellite local magnetic effects generally dominate the magnetometer readings. In the past, measurements were made remote enough to reduce the local effects and to simplify the

analysis procedures. This technique is no longer satisfactory with current requirements to measure small dipole moments. The remote measurements are limited as a result of background fluctuations which obscure the measurements, and from the lack of magnetometer sensitivity. Measurements must therefore be made at some intermediate distance and analysis techniques must be developed which are not hampered by any local effects that might still show up.

The test sequence starts when a zero magnetic environment has been set up within the facility reducing the possibility of interference from any induced magnetism that might occur. Next, recordings are made of the normal component of the magnetic field along the great circle in the xz -plane (horizontal plane). The curve begins with a measurement along the $+z$ axis and continues to $+x$, $-z$, $-x$, and back to $+z$. The turntable rotation is used to generate the curve. The satellite is then tilted through some given angle and a new recording is made beginning with $+z$. The process is repeated and more recordings are made until measurements have been made along the great circles of a sphere (the measurement sphere) as shown in Figure 4. The circles can be designated by a set of azimuth angles θ_i (tilt angles). Assume, for example, that the function

$$h(r, \theta, \varphi) = h(a, \theta, \varphi) = h(\theta, \varphi)$$

represents the normal component of the magnetic field on the measurement sphere of radius a . Then the family of measurement curves are the set of 1-dimensional functions

$$h(\theta_i, \varphi) = h_i(\varphi), \quad i = 1, 2, \dots, n$$

where n is the number of curves in the family.

Analysis Techniques

A computer program was devised to provide data to use in the study of analysis techniques. The program generates curves that would be obtained from measurements around given systems of symmetric multipole magnets. Specifications for a system of magnets are fed into the computer. Curves are then calculated and plotted representing the resulting magnetic field around the system. The program has the capability to vary certain parameters associated with the system of magnets, and then to generate families of curves representing the effects of these parameters. The program can also reduce each curve to its Fourier components if desired.

The mathematical models shown in Figure 5 are used to represent the individual magnets of a system. These models are used to simplify the mathematics for calculating the field around the system. Each arrow represents a dipole. The poles at the center of each magnet cancel, and the resulting configuration is identical to the one in the actual model.

Parametric Effects

A series of figures is presented to display the effects of certain parameters on measurements around dipoles in the xy -plane. The curves in each figure represent the normal component of the magnetic field around a circle with 4 foot radius in the xy -plane. Figure 6 shows a family of curves obtained by varying the dipole length L from 2 to 20 inches. The dipole moment was held constant. Figure 7 shows a family of curves generated by offsetting the dipole along the x -axis from 0 to $-1\frac{1}{2}$ inches. Figure 8 shows a family of curves resulting from dipole offsets along the y -axis from 0 to $-1\frac{1}{2}$ inches. The dipole for Figures 7 and 8 was 4 inches long. The axis of the dipole was parallel to the y -axis. Table 1 gives a comparison of the fundamental components of the individual curves. These were obtained from a numerical Fourier analysis. There is less than four percent variation in the amplitudes between curves from a 2 inch dipole and a 20 inch dipole measured at 4 feet. Families of curves similar to those in Figures 7 and 8, and based on actual measurements of a dipole, are given in [1].

The variation in the amplitudes of the fundamental components of the curves in Curve Families I and II (see Table 1) gives some indication of the accuracies to be expected when fitting a centered dipole to the measured data from near measurements. The fundamental component determines the direction and magnitude of the centered dipole which approximates the data with a least squares error. (Fourier analysis is a least squares approximation.) This suggests that the eccentricity or offset of a dipole should be considered when fitting the data as described by Chapman and Bartels² (p. 648). Of course if the curves were calculated for a greater measurement distance ($r \gg 4$ feet) then the fundamental components would show less variation. They would represent the magnitude and direction of the actual offset dipole more closely. This is one advantage of using remote measurements.

Torque Relationships

Before beginning any detailed discussion of basic analysis procedures it will be instructive to justify our concern with only the dipole component of the magnetism. This can be shown by investigating torque diagrams as shown in Figures 9 and 10. Figure 9 shows a diagram of the interaction between a dipole of moment $m(\vec{r}_1 - \vec{r}_2)$ and a uniform field of strength \vec{H} . The torque \vec{T}_D about some arbitrary point P is

$$\begin{aligned} \vec{T}_D &= \sum_{i=1}^2 \vec{r}_i \times \vec{F}_i = \vec{r}_1 \times (m\vec{H}) + \vec{r}_2 \times (-m\vec{H}) \\ &= m(\vec{r}_1 - \vec{r}_2) \times \vec{H} \end{aligned}$$

which is independent of P, as expected. Figure 10 shows a diagram of the interaction between a square quadrupole with poles of strength m, and the uniform field H. The torque T_Q about P is

$$\begin{aligned} T_Q &= \sum_{i=1}^4 \bar{F}_i \times \bar{F}_i \\ &= \bar{F}_1 \times (-m\bar{H}) + \bar{F}_2 \times (m\bar{H}) + \bar{F}_3 \times (-m\bar{H}) + \bar{F}_4 \times (m\bar{H}) \\ &= [(\bar{F}_2 - \bar{F}_1) + (\bar{F}_4 - \bar{F}_3)] \times m\bar{H} = 0 \end{aligned}$$

where $\bar{F}_i = m_i \bar{H}$ is the force vector acting on the *i*th monopole. T_Q is zero since the vectors $(\bar{F}_2 - \bar{F}_1)$ and $(\bar{F}_4 - \bar{F}_3)$ have equal magnitudes and are antiparallel. It can be shown likewise that the net torque on any higher order magnet is zero (in a uniform field). Therefore, only the dipole moment has to be determined to represent the satellite magnetism when torque equations are considered.

Monopole System

Consider a hypothetical system of N monopoles of pole strengths m_i and position vectors \bar{F}_i . Then the torque \bar{T} about the origin due to a uniform field of strength \bar{H} is

$$\bar{T} = \sum_{i=1}^N \bar{F}_i \times \bar{F}_i = \sum_{i=1}^N m_i \bar{F}_i \times \bar{H} = \bar{M} \times \bar{H} \quad (1)$$

where

$$\bar{M} = \sum_{i=1}^N m_i \bar{F}_i \quad (2)$$

is the effective dipole moment of the system about the origin. If

$$\sum_{i=1}^N m_i = 0 \quad (3)$$

then (1) and (2) are independent of the origin³. Let

$$\bar{R}_C = \sum_{i=1}^N |m_i| \left[\frac{\bar{F}_i}{\sum_{i=1}^N |m_i|} \right] \quad (4)$$

be the "magnetic center C" of the system and let

$$\bar{F}'_i = \bar{F}_i - \bar{R}_C$$

Then

$$\bar{M} = \sum_{i=1}^N m_i \bar{F}_i = \sum_{i=1}^N m_i \bar{F}'_i + \left(\sum_{i=1}^N m_i \right) \bar{R}_C \quad (5)$$

If (3) does not hold then \bar{M} consists of two terms as shown in (5). The first term on the right represents the net dipole moment of the system about the magnetic center. The second term represents the monopole moment relative to the origin. Assume for example that all the monopoles are positive or all are negative. Then

$$\left(\sum_{i=1}^N m_i \right) \bar{R}_C = \left(\sum_{i=1}^N m_i \right) \left(\frac{\sum_{i=1}^N m_i \bar{F}_i}{\sum_{i=1}^N m_i} \right) = \sum_{i=1}^N m_i \bar{F}_i$$

and (5) implies

$$\sum_{i=1}^N m_i \bar{F}'_i = 0.$$

Therefore the moment of the system results strictly from the monopole moment. (The dipole moment relative to the magnetic center is zero.) Of course the problem still remains of finding the proper system of monopoles. This could be difficult since in general there is no unique system based solely on the measured data.

Basic Dipole Moment Calculations

Procedures for calculating the resultant dipole moment from measured data can be relatively simple, depending on the complexity of this data. If the measurements were made around a large enough sphere, then geometric effects and the field from high order magnets would be greatly reduced relative to the field from the dipole. Figure 11 shows fall-off curves for the axial field from magnets with equal pole strengths and equal diameters or lengths. No particular units were used. Figures 12 and 13 show a comparison between near and remote fields around a system of five dipoles with different locations and orientations. The near field was computed for a radius of 4 feet and the remote field for 40,000 feet. Curves from the remote measurements reduce to simple sine waves representing the field from the resultant dipole. The components of the resultant dipole moment of the system can be calculated from the sine curves. The calculations are described below using curves from a known dipole. Only the curves for two perpendicular planes are necessary to determine the magnitude and direction of the dipole.

Curves were computed to represent the normal component of the field around the dipole illustrated in Figure 14. Figure 15 displays the curves for a measurement sphere of 4 foot radius. The curves for the xy- and the xz-planes are used to demonstrate the procedures for calculating the components of the dipole moment vector \bar{M} where

$$\bar{M} = (M_x, M_y, M_z)$$

in rectangular coordinates. From each curve we determine the amplitude and phase angle as shown in Figures 16 and 17. This gives

$$\begin{aligned}
 H_{xy} &= 0.400 \text{ gamma} \\
 \theta_{xy} &= 30.0^\circ \\
 H_{xz} &= 0.417 \text{ gamma} \\
 \theta_{xz} &= 33.7^\circ
 \end{aligned}$$

(These values were determined accurately from a numerical Fourier analysis.) The components are calculated from the following approximate relationships.

$$\begin{aligned}
 M_x &= (H_{xy} \cos \theta_{xy} r^3) / 2 \\
 M_y &= (H_{xy} \sin \theta_{xy} r^3) / 2 \\
 M_z &= (H_{xz} \sin \theta_{xz} r^3) / 2
 \end{aligned}$$

where

$$r = 122 \text{ cm (4 feet).}$$

H_{xy} and H_{xz} are in gauss. This gives

$$\begin{aligned}
 M_x &= 3.14 \text{ gauss - cm}^3 \\
 M_y &= 1.82 \text{ gauss - cm}^3 \\
 M_z &= 2.10 \text{ gauss - cm}^3
 \end{aligned}$$

The spherical representation of the vector, (M, θ, φ) , can be calculated as follows:

$$M = (M_x^2 + M_y^2 + M_z^2)^{1/2} = 4.20 \text{ gauss - cm}^3$$

$$\theta = \theta_{xy} = 30^\circ$$

$$\varphi = \cos^{-1}(M_z/M) = 60^\circ$$

where M is the resultant moment, θ is the azimuth angle, and φ is the zenith angle.

Opposing Dipoles

Figure 18 is given to show the field resulting from two equal and opposite dipoles. Their positions are shown in the diagram. The geometry of the dipoles represents a situation that might arise in a test in which the dipole moment of a spacecraft (centered dipole) has been compensated by a dipole attached to the outside of the craft. The condition results in a zero net torque when a uniform external field is applied, but this is not obvious from a study of the resulting curve. Figure 19 displays the first six Fourier components of the curve including the constant component. The fundamental or "dipole" component is not zero implying that a harmonic analysis will not give the desired result. Therefore, more information is needed along with more sophisticated analysis techniques.

Another implied result of this example relates to the possibility of approximating the data with the field from an offset dipole by the method of least squares error as previously mentioned. In a least squares approximation the dipole position, direction, and magnitude are allowed to vary. The desired resultant dipole in this example is zero since the torque would be zero. But the implication is that the offset dipole determined by the least squares approximation would be non-zero. This follows from the fact that the centered dipole from the Fourier analysis is a special case of an offset dipole approximation. Therefore the offset dipole determined by least squares would necessarily approximate the data as good as or better than the centered dipole. Therefore the curve from the offset dipole would have an amplitude other than zero which is not the desired result.

Since the centered dipole method and the general offset dipole method have both failed to give the desired result, an additional step might prove helpful. Some means should be devised to specify the dipole position prior to applying the method of least squares approximation. Then only the dipole direction and magnitude are allowed to vary. Chapman and Bartel² (page 648) define the dipole position as the magnetic center, and give a method for finding it.

Miscellaneous Methods

Some analysis techniques are presently being evaluated with the aid of a computer. In one method near field measurements are used as a basis for an extrapolation process which defines the field on a sphere of large diameter. The dipole may then be estimated by applying the method described above to the remote field values calculated from the extrapolation process. One method of performing the extrapolation would involve the numerical solution of the Neumann problem^{4,5} using the measurement data as the boundary condition. The solution gives the potential at any point outside the sphere. We can determine the field at points on a large sphere, say 10^4 times greater than the measurement sphere. On this large sphere the ratio of the quadrupole field to the dipole field will be 10^{-4} times the value on the measurement sphere. The ratio for higher order multipoles will be even smaller.

A study of the components of spherical harmonics may also result in a practical solution of the problem since each harmonic represents the potential from a multipole magnet of an orthogonal system of magnets, i.e., monopole, dipole, quadrupole, etc. This analysis would involve the determination of the harmonic coefficients of the second harmonic. In this case an extrapolation process is unnecessary. Chapman and Bartel² (page 631) describe a method for the numerical calculation of the spherical harmonic coefficients. A close study of the

data in Figures 7, 8, 18, and 19 and in Table 1 seems to imply that the dipole component in the spherical harmonic analysis is not the one desired. If it were then the amplitudes of the fundamental components in Curve Families I and II in Table 1 would all be identical. And in Figure 19 the fundamental component would be zero.

Another method being studied is to define a system of pure monopoles or dipoles which represents the measured data. Fictitious magnets are located on the surface of a small sphere within and concentric to the measurement sphere. This system can be used to calculate the resultant dipole directly or to provide a basis for the extrapolation process mentioned above. The sphere of magnets can best be described as follows. Locate a magnet at each measurement point on the measurement sphere. If a system of dipoles is used then place the center of a dipole at each measurement point and align the dipole axis normal to the sphere. Now shrink the sphere to the prescribed diameter of the magnet sphere. The polarity and moment (or pole strength for monopoles) for each magnet is determined by fitting a unit system (magnets of unit moment) to the measured data points by the numerical method of least squares or from the solution of simultaneous linear equations. Figure 20 shows the xy-plane for a system of dipoles. As shown in equation (2) the effective dipole moment of a system of monopoles or dipoles can be calculated simply by summing over all the products of the position vectors and the pole strengths of the poles.

Results and Conclusions

Other methods for estimating the effective dipole moment, or the net torque produced by an external magnetic field, have been devised. Toesman^o describes a method for measuring each of the three components of the dipole moment. In this method the satellite is suspended from a cable along an axis perpendicular to the component to be determined. A pulsing magnetic field is applied in a horizontal direction which is also perpendicular to the unknown component. The square-wave field produces a rotational oscillation with steadily increasing amplitude. The dipole component is determined from its relationship to the applied field and to the rate of increase in the amplitude of the oscillation. The other two components are determined similarly.

Another method, to be tested at the Goddard Space Flight Center (NASA), consists of the direct measurement of the torque on a satellite in an applied field. The satellite is floated on a fluid, and the torque is determined by measuring the increase in tension on a restraining wire when the external field is applied. Each of the torque components along the two horizontal axes is determined by applying a field perpendicular to each axis and noting the increase in tension in the wire. The craft is then tilted

90° and the component along the third axis is measured.

The study presented here is not complete. Numerical methods should be devised for fitting an offset dipole, a system of monopoles, and a system of magnets to the measured data. Investigations should be made to determine the required accuracy for the measuring instruments and for the positions of the measurements. Considerable information may be obtained using a computer program which calculates the field around a dipole (or system of symmetric magnets). Slight angular offsets can be introduced into the calculated data to simulate errors in measurement positions. Also the numerical values of the data can be truncated to simulate the instrument inaccuracies.

The method described in this paper is based on the measurement and analysis of the normal component of the magnetic field on a sphere surrounding the satellite. The measurements are made without the application of a net external field, and are used to estimate the resultant dipole moment. The necessity of gimballing the craft could present problems with the accuracy of the measurement positions. Nevertheless, measurements are not sensitive to normal air currents, and the setup and measurement time is relatively short. The method involves the use of a high-speed computer and indicates the feasibility of developing improved techniques of analysis.

Bibliography

1. Lackey, M. H., Magnetic Moment Testing of Satellites (U, U.S. Naval Ordnance Laboratory Technical Report No. 64-52 (18 Jan 1965))
2. Chapman, S., and J. Bartels, Geomagnetism (Oxford University Press, Oxford, England, 1940), Vol. II, pp. 543-1049
3. Landau, L., and E. Lifshitz, The Classical Theory of Fields (Addison-Wesley Publishing Company, Inc., Reading, Massachusetts, 1951), (Translated from the Russian by Morton Hamermesh), Chap. 5, p. 103
4. Webster, A. G., Partial Differential Equations of Mathematical Physics (G. E. Steckert and Company, New York, 1933), 440 pp
5. Bramble, J. H., Numerical Solution of Partial Differential Equations (Academic Press, New York and London, 1967), 373 pp
6. Toesman, B. E., Resonance Technique for Measurement of Satellite Magnetic Dipole Moment, Proceedings of the Magnetic Workshop, NASA Technical Memorandum No. 33216, (30 Mar 1965), pp. 125-138

X_1 or Y_1 (inches)	AMPLITUDE (GAMMA)	
	FAMILY I	FAMILY II
0	7.24	7.24
-2	7.25	7.27
-4	7.28	7.36
-6	7.33	7.51
-8	7.40	7.72
-10	7.49	8.01
-12	7.60	8.38
-14	7.75	8.85

L	LENGTH VARIATION
2	3.798
4	3.802
6	3.809
8	3.818
10	3.831
12	3.846
14	3.864
16	3.885
18	3.909
20	3.936

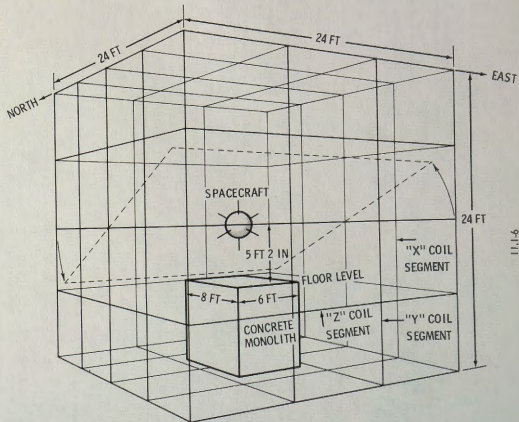


Fig. 1 DIAGRAM OF COIL SYSTEM

TABLE 1 AMPLITUDE OF FUNDAMENTAL COMPONENTS
IN CURVE FAMILY

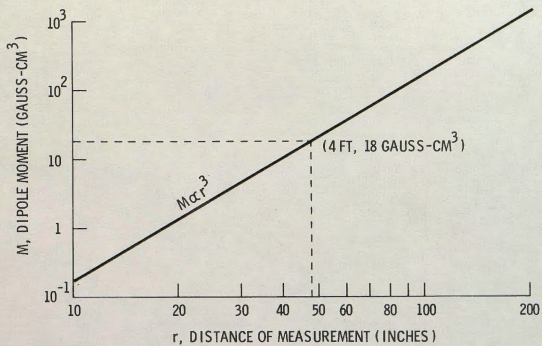


Fig. 2 MINIMUM DETECTABLE DIPOLE FOR SENSITIVITY OF 4 GAMMA

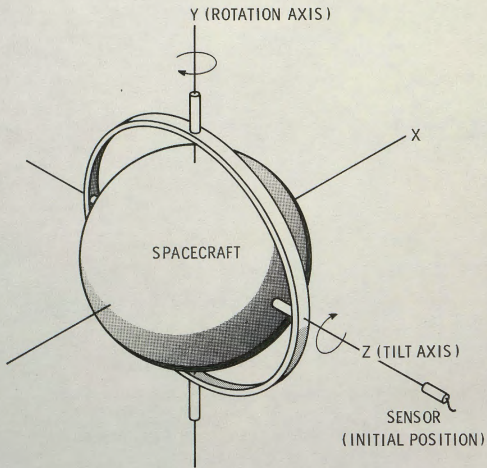


Fig. 3 DEGREES OF FREEDOM FOR MEASUREMENTS

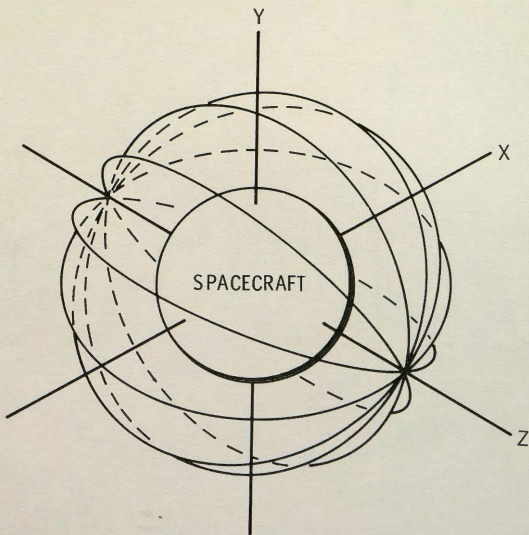
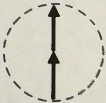
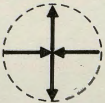



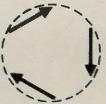


Fig. 4 SPHERE OF MEASUREMENTS

	DIPOLE	QUADRUPOLE	HEXAPOLE
MATHEMATICAL MODEL			
ACTUAL MODEL			

ARROWHEAD INDICATES NORTH POLE

Fig. 5 MODELS OF MAGNETS

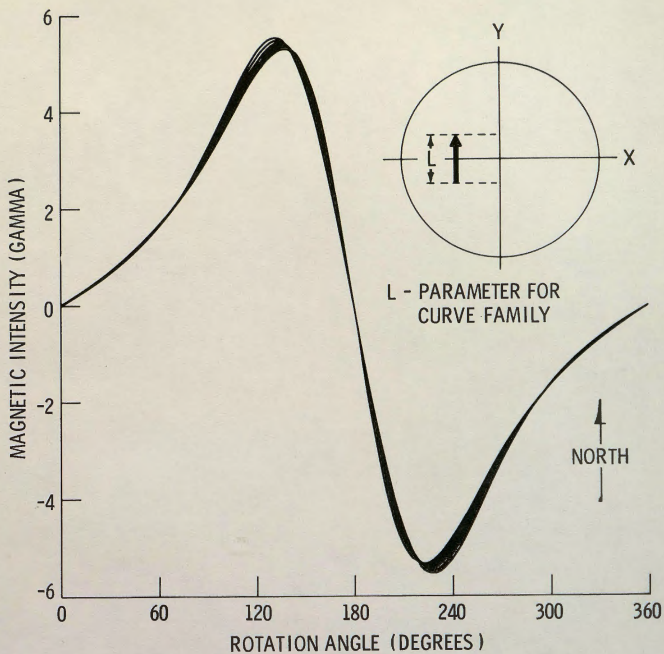


Fig. 6 DIPOLE LENGTH VARIATION WITH CONSTANT MOMENT

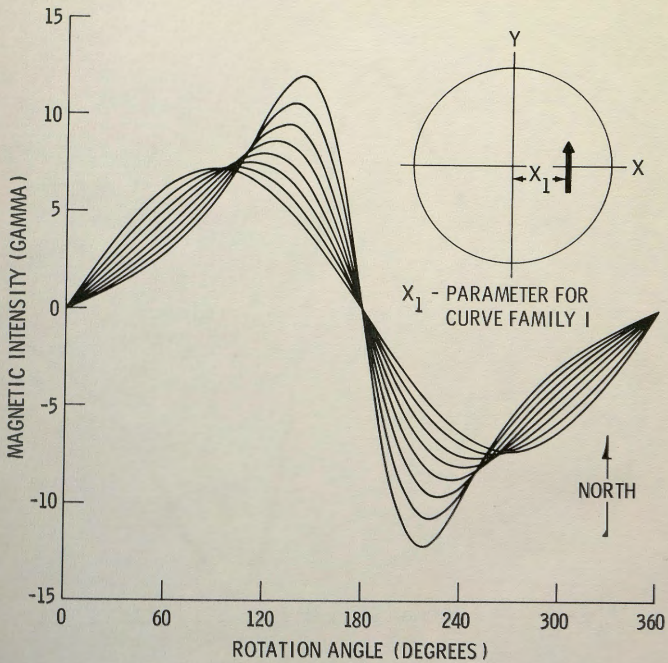


Fig. 7 CURVE FAMILY I

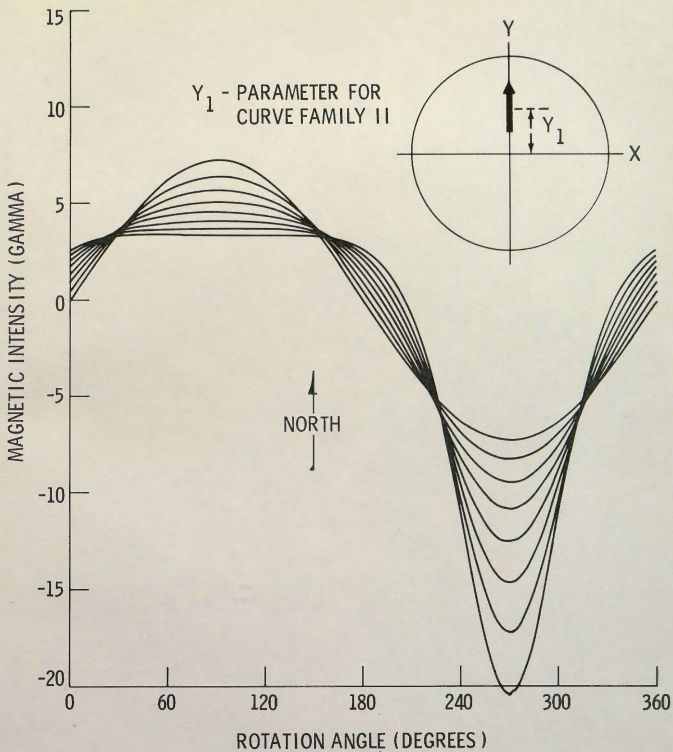
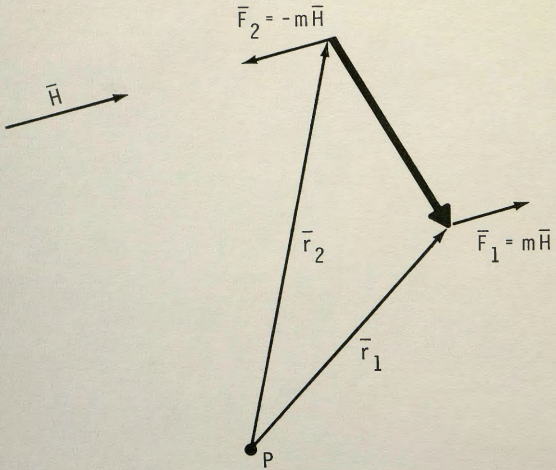


Fig. 8 CURVE FAMILY II



$$\vec{T}_D = (\vec{r}_1 - \vec{r}_2) \times m\vec{H}$$

Fig. 9 TORQUE DIAGRAM FOR DIPOLE

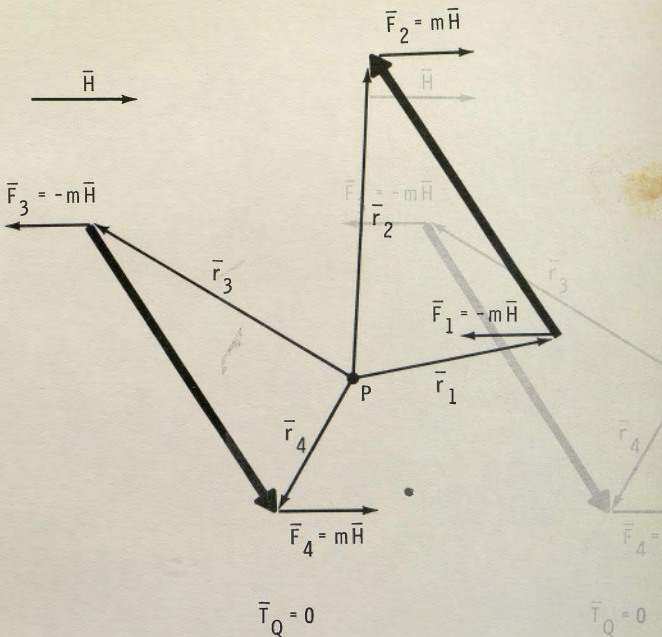


Fig. 10 TORQUE DIAGRAM FOR QUADRUPOLE TORQUE DIAGRAM

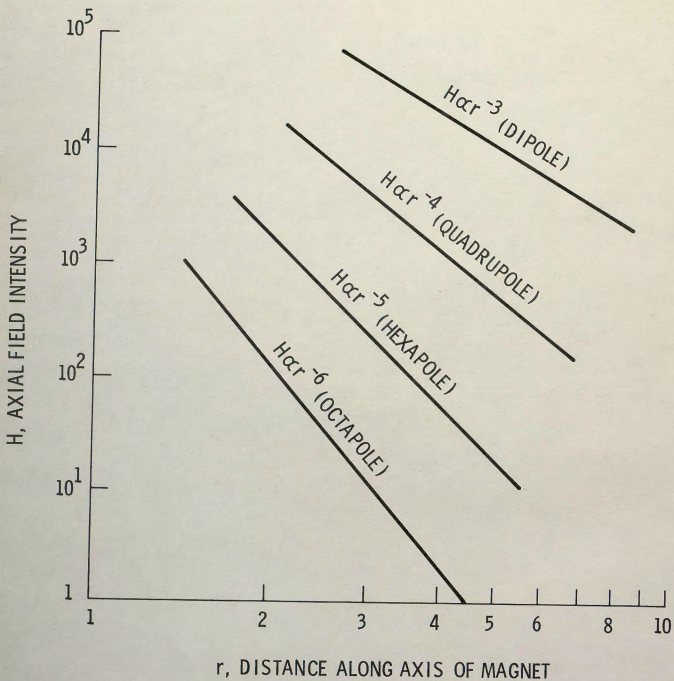


Fig. 11 FALL-OFF OF AXIAL FIELD OF MAGNETS

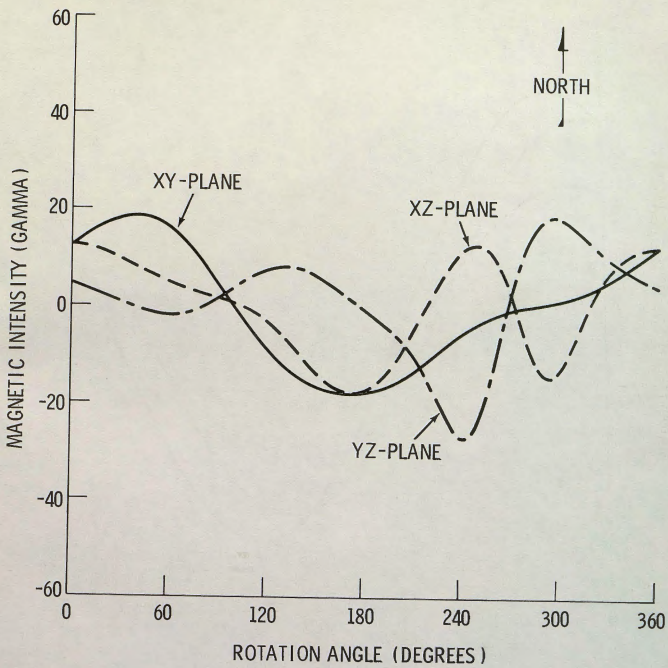


Fig. 12 NEAR FIELD OF SYSTEM OF 5 DIPOLES

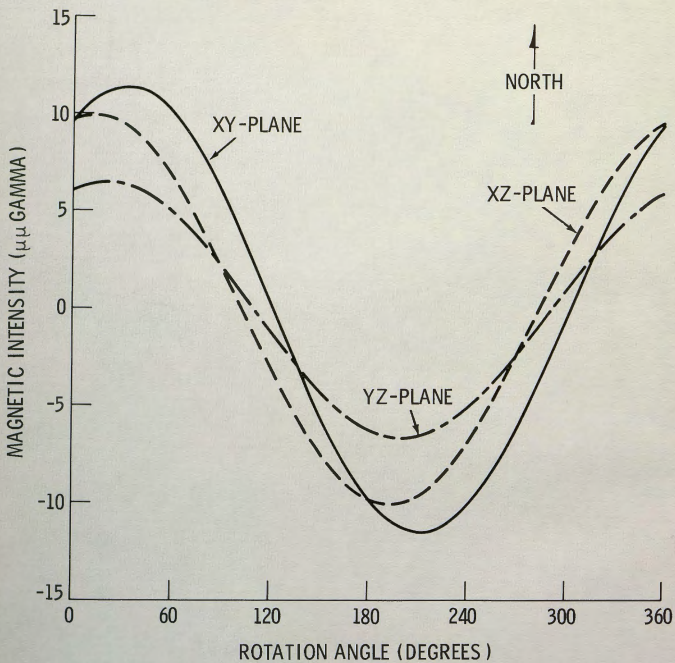


Fig. 13 FAR FIELD OF SYSTEM OF 5 DIPOLES

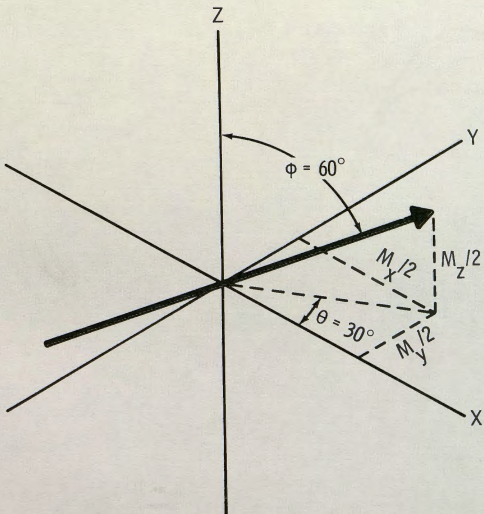


Fig. 14 DIPOLE COORDINATES

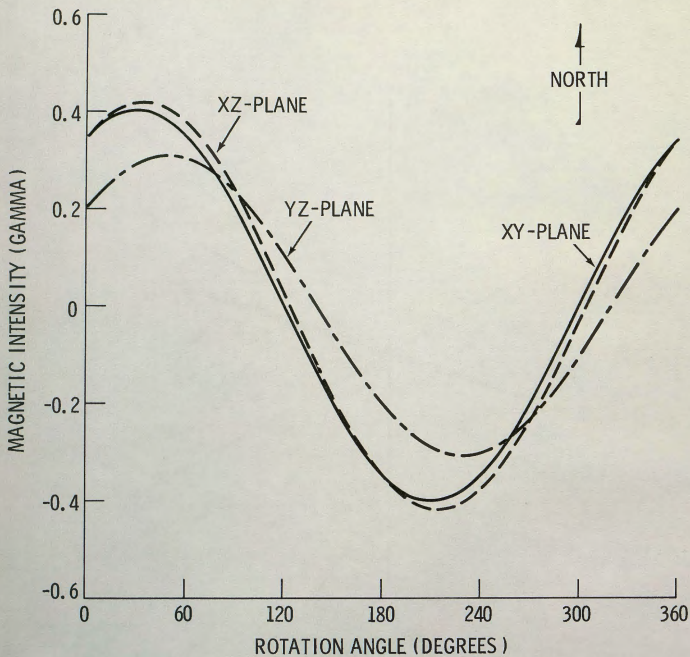


Fig. 15 RADIAL FIELD AROUND DIPOLE

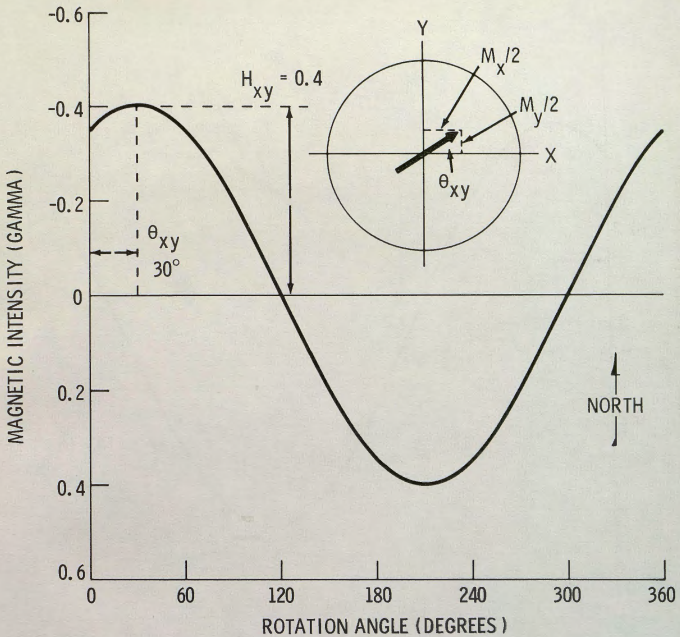


Fig. 16 RADIAL FIELD IN XY-PLANE

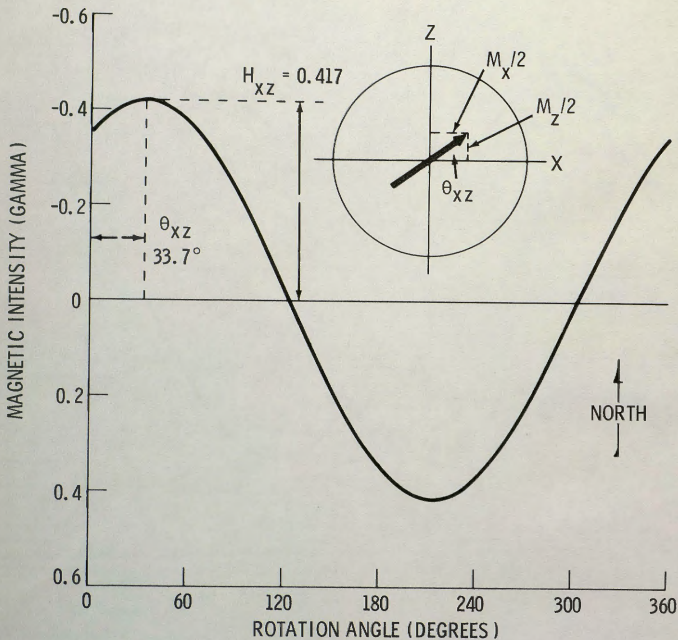


Fig. 17 RADIAL FIELD IN XZ-PLANE

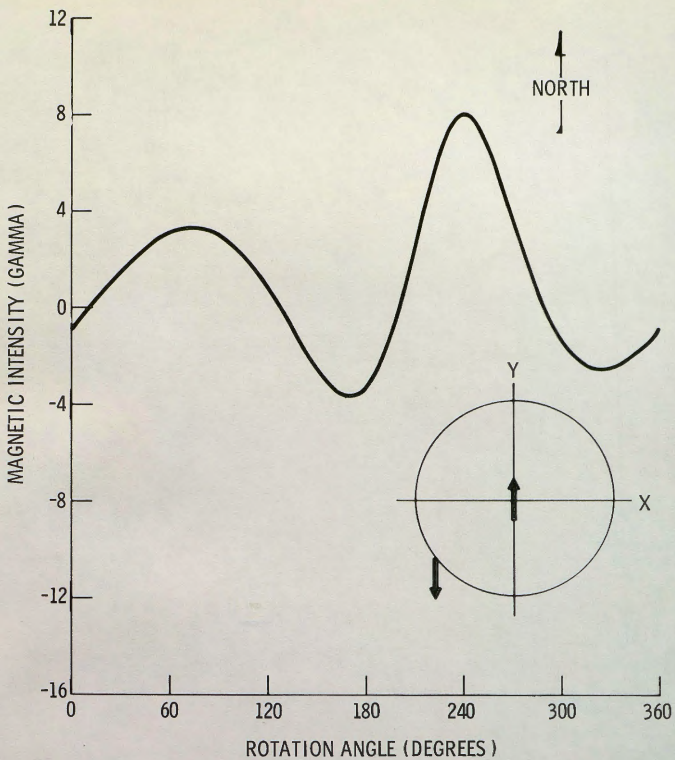


Fig. 18 OPPOSING DIPOLES

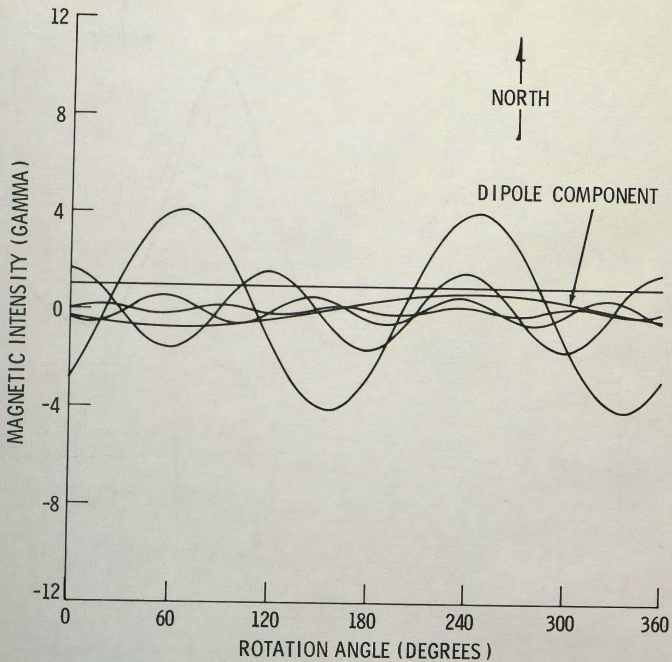


Fig. 19 FOURIER COMPONENTS FOR OPPOSING DIPOLES

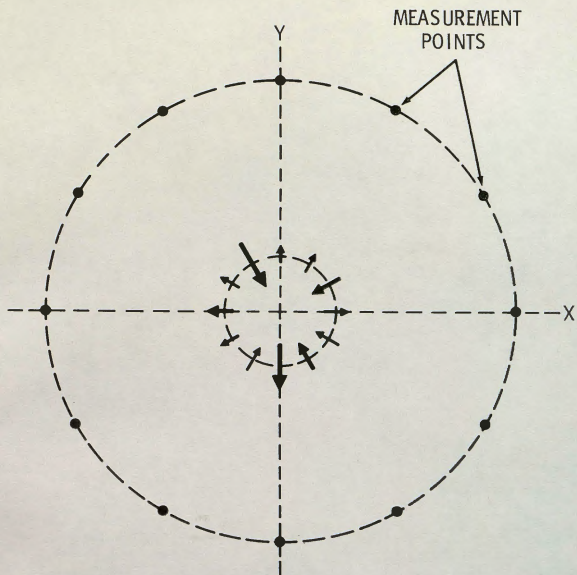


Fig. 20 APPROXIMATING SYSTEM OF DIPOLES
XY-PLANE